THE RELATIVE SPECTRAL RESPONSE CALIBRATION OF THE ISO-SWS

B. Vandenbussche[1], P. W. Morris[2], E. A. Valentijn[3], D. A. Beintema[4], D. R. Boxhoorn[3], L. Decin[1], T. de Graauw[4], H. Feuchtgruber[5], A. M. Heras[6], F. Lahuis[4], R. Lorente[7], D. Lutz[5], P. R. Roelfsema[4], A. Salama[7], R. F. Shipman[4], R. Van Malderen[1] and E. Wieprecht[5]

[1]Katholieke Universiteit Leuven, Instituut voor Sterrenkunde, Celestijnenlaan 200B, B-3001 Leuven, Belgium
[2]IPAC, Passadena, USA
[3]Kapteyn Lab, Groningen, The Netherlands
[4]SRON Laboratory for Space Research, Groningen, The Netherlands
[5]MPE, Garching, Germany
[6]Astrophysics Division of ESA, ESTEC, Noordwijk, The Netherlands
[7]ISO Data Centre, Astrophysics Division, ESA, Villafranca del Castillo, Spain

ABSTRACT

The Relative Spectral Response Function (RSRF) characterises the wavelength dependent response of a spectrometer. The wavelength range of the grating section of the ISO-SWS is covered in 15 spectral bands for each of which the RSRF has to be determined.

We discuss how the RSRF was measured during the Instrument Level Tests before launch, and how it was corrected based on in-orbit measurements of stellar calibration sources.

Uncertainties in synthetic spectra and noise in the calibration observations can result in the introduction of erroneous spectral features in the RSRF. We show how this can be avoided by a careful selection of calibration sources across different spectral types and the use of spline smoothed correction curves.

Key words: ISO – SWS – Calibration – Relative Spectral Response Function – RSRF – Flux calibration

1. INTRODUCTION

The grating section of the Short Wavelength Spectrometer SWS (de Graauw et al. 1996) on-board the Infrared Space Observatory ISO (Kessler et al. 1996) covers the wavelength range between 2.36 μm and 45 μm in 15 overlapping spectral channels. Each of these channels, the so-called AOT-bands, are characterised by a unique combination of the instrument aperture, the grating order, the detectors used and a set of order selection filters in the light path. Therefore every detector has a different Relative Spectral Response Function (RSRF) in every AOT-band. In every AOT-band a block of 12 detectors is used hence the complete RSRF behaviour of the SWS instrument is characterised by 12×15 RSRF functions.

2. RSRF MEASUREMENTS BEFORE LAUNCH

Prior to launch, the RSRF was determined during the lab tests on instrument level (ILT) (Feuchtgruber et al. 2003). The measurements consisted of SWS spectra of a blackbody calibration source at full spectral resolution, fully sampled in every detector. Several scans were performed through the different SWS apertures and with different blackbody temperatures. The spectra obtained were then divided by a Planck function of the corresponding blackbody temperature to obtain the RSRF. Figure 1 illustrates this calibration process.

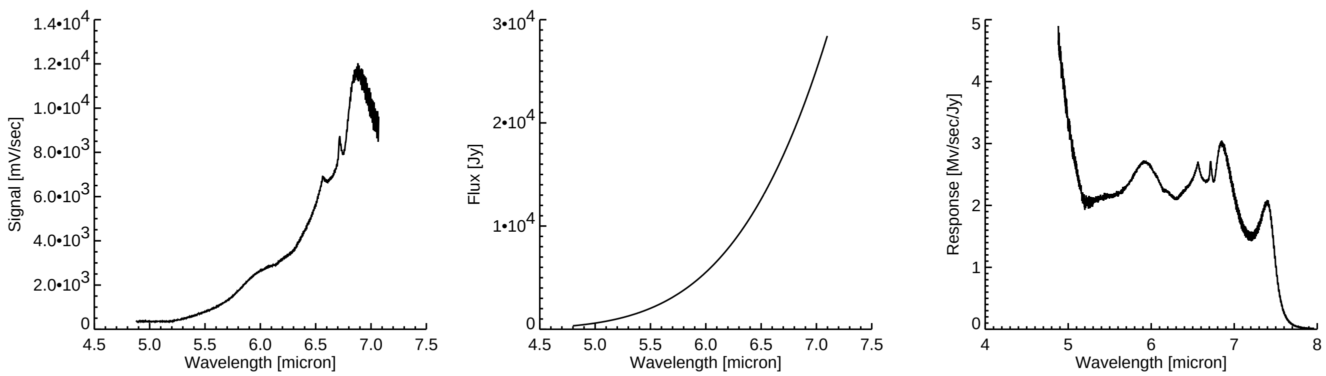

Figure 1. Determining the RSRF from pre-launch SWS measurements of a blackbody in the lab. The left panel shows the response of an SWS detector during a scan in AOT-band 2b of a 173K blackbody. The middle panel shows a Planck curve for this blackbody temperature. The right panel shows the division of the two. This is the Relative Spectral Response for this detector in AOT-band 2b.

Proceedings of the Conference "The Calibration Legacy of the ISO Mission", VilSpa, Spain, February 2001
ESA SP-481, 2003, eds. L. Metcalfe, A. Salama, S. B. Peschke & M. F. Kessler

3. IN-ORBIT VERIFICATION OF THE ILT RSRF

After launch, the accuracy of the ILT RSRF was verified by comparing SWS observations to synthetic spectra, composite spectra or template spectra for various sky calibration sources. This comparison revealed both broadband errors and small-scale errors.
Figure 2 shows the broadband differences between a composite spectrum by Cohen et al. (1992) and an SWS observation of Sirius.

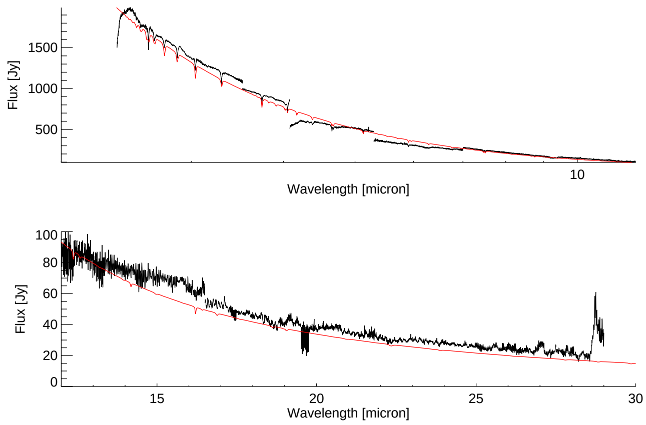

Figure 2. Comparison of a composite by Cohen et al. and the SWS spectrum of Sirius. The spectrum was calibrated with the RSRF derived from the pre-launch blackbody scans.

The beam from the source used during the pre-launch measurements filled the slit of the SWS entirely. Therefore the RSRF measured during these tests has a slightly lower spectral resolution than observations of point-like sources in-orbit. We can see this in band 3, where the fringes caused by the Fabry-Pérot effect of a layer on the back-illuminated detectors are sharper in observations of point-like sources than in the RSRF. As shown in Figure 3 this is also apparent in bands 1 and 2: the fringes originating from spectral order selection filters are hardly resolved in the RSRF while they are resolved in high-resolution

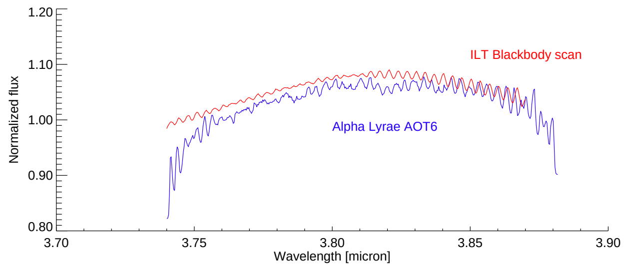

Figure 3. In full-resolution scan AOT6 observations of point-like sources the fringes (here in off-band data band 1D) are better resolved than in the ILT blackbody scans.

spectra of stars. This puts a hard limit on the S/N that can be achieved with the ISO-SWS at full spectral resolution.

4. POLYNOMIAL BROADBAND CORRECTION

Several effects, e.g. leaks in laboratory setup filters and uncertainties or small drifts in the blackbody temperature, can be responsible for the broadband errors in the pre-launch RSRF.

The SWS RSRF has been corrected for broadband differences between in-orbit observations and reference spectra. The quality of this correction improved in the course of the project as more SWS spectra of calibration stars were observed and the reference spectra available became more accurate.

Already early in the mission (May 1996) an RSRF correction for the apparent fall-off on the blue side of AOT-bands 1A and 2A was implemented. This correction was a polynomial fit (n=2) to the division of an SWS spectrum of α Lyrae and a Kurucz synthetic spectrum by Cohen et al. (1992). Figure 4 shows the difference between the ILT RSRF for band 1a and the RSRF after correction with a second order polynome fitted as described above.

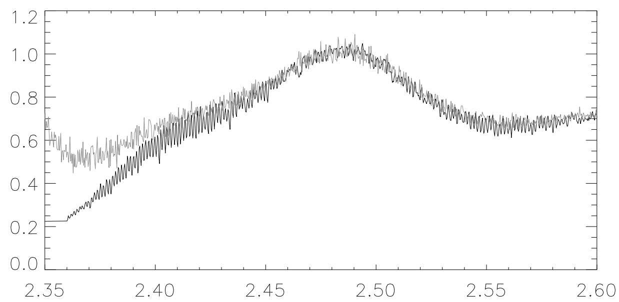

Figure 4. The difference between the band 1A ILT RSRF (black) and the RSRF corrected with a polynomial fit (n=2).

Later (March 1997) this method was also applied to correct for more subtle residues in other AOT-bands. By that time more SWS observations of stellar calibrators were available, covering early and late spectral types.

5. SPLINE SMOOTHING OF RESIDUES

Fitting polynomes to the residues was clearly not optimal for the variety of shapes showing up in the residues. The problem with polynomial fits is that a local bias always translates to a global bias, e.g. strong oscillations in the high-order polynomial fit to noisy data. We therefore adopted a method of smoothing the residues with a cubic spline.

A spline function $S^{(m)}$ of order m with knots x_i, $i = 1..k$ is a set of functions F_j, $j = 1..k-1$ that are defined over the intervals $[x_0,x_1]$, ... $[x_{k-1}, x_k]$ and stitched together in the knots so that the combined function S^m is m times continuously differentiable at the knots. The functions F_j are often cubic polynomes (n=3). We then talk about cubic splines.

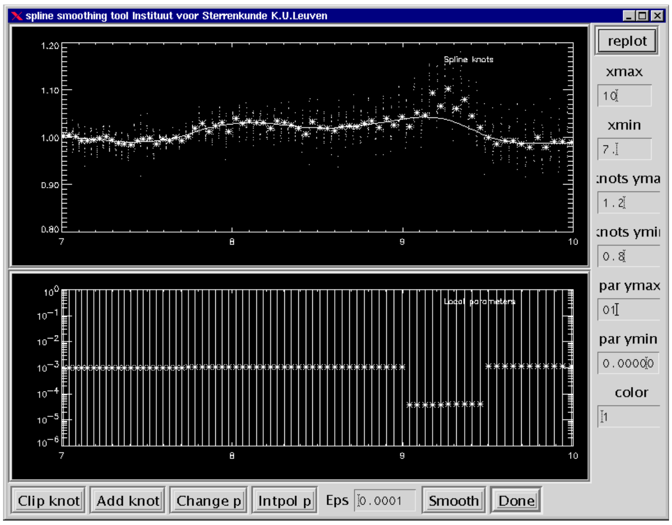

Figure 5. The spline smoothing widget allows fitting of only the features that are understood to be instrumental. The upper panel shows the residues (dots), the averaged residues (asterisks) that are the knots k_i for the smoothing spline (solid line). The lower panel shows the parameters s_i attributed to the knots k_i.

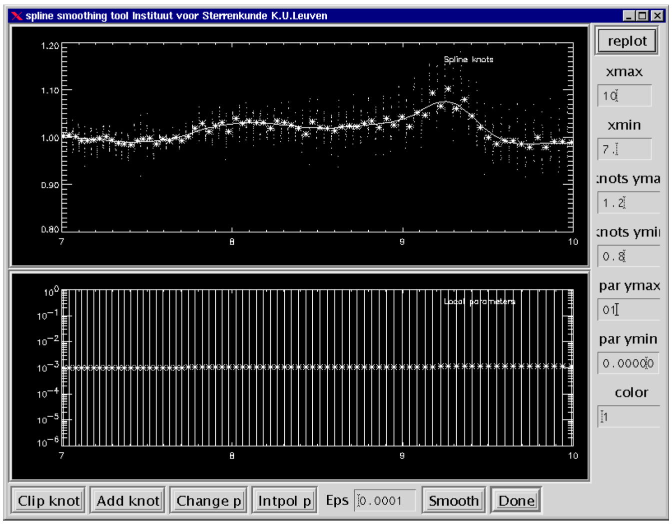

Figure 6. After verification on many sources, the 9.3 feature in band 2C spectra was understood as an error in the RSRF. The smoothing spline was then allowed to follow the shape of the feature accurately.

Spath (1995) describes various algorithms to smooth a dataset using splines. We have adopted an algorithm to smooth a dataset (x_i, y_i), $i = 1, .., k$ by determining a cubic spline $S^{(2)}$ for which $w_i(S^{(2)}(x_i) - y_i)^2 < P_i, i = 1, ..., n$. w_i are weights for the data points and P_i is a parameter for the smoothness in knot k_i. w_i and S_i are combined into one knot parameter s_i. Varying this parameter in a knot will result in a smoothing spline which is more 'stiff' or which follows the dataset more accurately in that region.

Cubic spline smoothing allows to make the correction curve follow the features in the residues where they are understood to be instrumental. In regions where the residues are believed to be unreliable (less accurately modelled features in the synthetic spectra, etc...) the spline smoothing curve is forced to be more 'stiff'. Therefore it is necessary that one understands the strong and weak points in the reference spectra and datasets used.

This method was implemented for every AOT-band and every detector as follows : for a selected set of calibration sources and reference spectra we calculated residues $[observation/model]$. These residues are averaged over bins of $\lambda/\delta\lambda$=200). The data points in the average residue are then taken as the knots for a cubic spline smoothing. We tune the local stiffness of the smoothing spline in an Interactive Analysis widget tool, and the resulting spline is then evaluated in the wavelengths sampled in the ILT RSRF. These factors are multiplied with the responses in the ILT RSRF to obtain the corrected RSRF.

The spline smoothing widget allows to lower the knot parameters of the knots in regions where features in the residues are not understood to be instrumental. No correction for such features will be applied to the RSRF (Figure 5).

After carefully studying many sources observed by the SWS, four features in the residues (9-9.3, 10.1, 11.0 μm in band 2C and at 12.3μm in band 3A) were understood as inaccuracies in the RSRF, e.g.the result of a strong memory effect while scanning over a feature in the RSRF during the ILT tests. Therefore, the smoothing spline is allowed to be less 'stiff' in this region and follows the shape of the knots. Figure 6 shows this for the feature at 9.3 μm.

6. REFERENCE SPECTRA SELECTION

Different reference spectra for stellar calibration sources in the Mid-infrared are available. Their reliability depends on many aspects like the underlying star model - e.g. LTE Kurucz models may be appropriate for early type stars, but for cool giants the non-LTE MARCS code of the Uppsala group is more appropriate. Other aspects resulting in different reliabilities are the adopted abundances and fundamental stellar parameters and the atomic and molecular line lists used in the generation of the synthetic spectra. Figure 7 shows how the shape of the SiO fundamental band differs in different reference spectra for α Bootis (K1.5 III). We see that the band is not present in the synthetic spectrum based on a Kurucz model by Hammersley et al. (1998) and the MARCS synthetic spectrum by van der Bliek et al. (1998) while the composite by Cohen et al. (1992) and the MARCS synthetic spectrum by Decin (2000) both show the band. The difference between the two synthetic spectra based on the MARCS code is primarily due to the difference in line lists used.

7. CALIBRATION SOURCES

The calibration sources were selected to cover a wide diversity in spectral types. This allowed avoidance of biases to spectral features typical for different spectral classes. The RSRF used in the processing of the ISO legacy archive (OLP 10) have been corrected using the stars in table 1. For the short

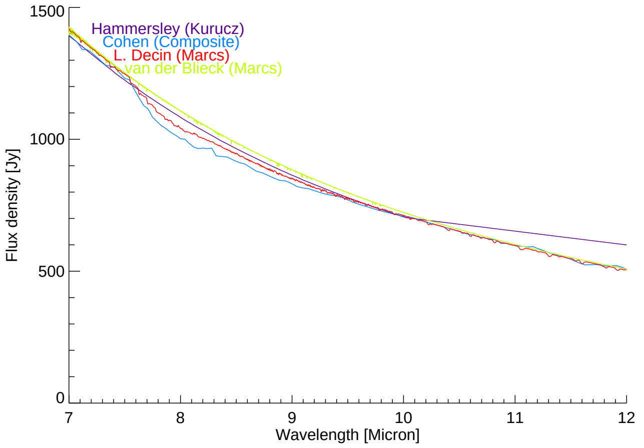

Figure 7. Example of the differences in synthetic spectra and a composite for α Bootis.

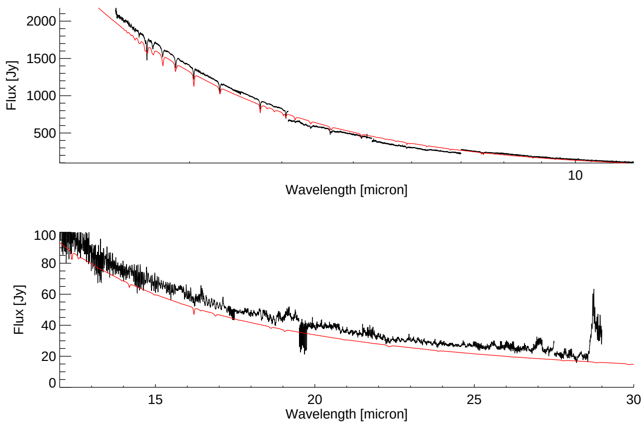

Figure 8. Comparison of a composite by Cohen et al. and the SWS spectrum of Sirius. The spectrum was calibrated with the corrected RSRF as in OLP 10.

Table 1. The calibration sources for the corrections of the RSRF in OLP 10, the version of the ISO data reduction pipeline used for the legacy archive.

Source	HR	Spectral type	Wavelength range
α Lyr	HR 7001	A0V	2.3μm - 30μm
α CMa	HR 2491	A1V	2.3μm - 30μm
β Leo	HR 4534	A3 V	2.3μm - 4μm
α Car	HR 2326	F0 II	2.3μm - 12μm
α Cen A	HR 5459	G2 V	2.3μm - 30μm
δ Dra	HR 7310	G9 III	2.3μm - 12μm
ξ Dra	HR 6688	K2 III	2.3μm - 12μm
α Boo	HR 5340	K1.5 III	2.3μm - 45μm
β UMi	HR 5563	K4 III	2.3μm - 12μm
γ Dra	HR 6705	K5 III	2.3μm - 30μm
α Tau	HR 1457	K5 III	2.3μm - 30μm
HD 149447	HR 6166	K6 III	2.3μm - 12μm
β And	HR 337	M0 III	2.3μm - 30μm
α Cet	HR 911	M2 III	2.3μm - 30μm
β Peg	HR 8775	M2.5 III	2.3μm - 30μm

wavelength section ($< 12\mu$m) we used synthetic spectra based on MARCS models by Decin (2000). For the long-wavelength section, composites by Cohen et al. (1992) were used.

Figure 8 shows the SWS spectrum of sirius as processed with OLP 10 for the legacy archive. Compared to figure 2 the broadband shape is remarkably more reliable, especially in the short wavelength section.

8. CONCLUSION

Characterisation of the RSRF during pre-launch laboratory tests on instrument level have been necessary to calibrate the RSRF of the ISO-SWS acurately. Limited S/N in the observations and limited reliability of the strength and shape of spectral features in synthetic spectra prohibit the use of in-orbit data to determine the small-scale structure of the RSRF.

The broad scale inaccuracies in the SWS ILT RSRF have been successfully corrected with a smoothed spline fit to the differences between in-orbit observations and reference data. The method of spline smoothing corrections is robust against inaccurate reference data as long as the sources show a variety of spectral features and the reference data a variety in inaccuracies.

REFERENCES

Cohen, M., Walker, R. G., Barlow, M. J., and Deacon, J. R., 1992, ApJ, 104, 1650

de Graauw, T., Haser, L. N., Beintema et al., 1996, A&A, 315, L49

Decin, L., 2000, Ph.D. thesis, Katholieke Universiteit Leuven

Feuchtgruber, H., Katerloher, R., Jakob, G. et al., 2003, this volume

Hammersley, P. L., Jourdain de Muizon, M., Kessler, M. F. et al., 1998, A&A Supplement, 128, 207

Kessler, M. F., Steinz, J. A., Anderegg et al., 1996, A&A, 315, L27

Späth, H., 1995, One dimensional spline interpolation algorithms

van der Bliek, N. S., Morris, P. W., Vandenbussche, B. et al., 1998. In: IAU Symp. 189: Fundamental Stellar Properties, Vol. 189, 89